

Electronic Supplementary Information for

Structure-designed synthesis of FeS₂@C yolk-shell nanoboxes as a high-performance anode for sodium-ion batteries

Zhiming Liu^{a‡}, Tianchi Lu^{a‡}, Taeseup Song^c, Xin-Yao Yu^d, Xiong Wen (David) Lou^{b*}, Ungyu Paik^{a*}

^a Department of Energy Engineering, Hanyang University, 222 Wangsimni-ro, Seongdong-gu, Seoul, 04763, Korea. E-mail: upaik@hanyang.ac.kr

^b School of Chemical and Biomedical Engineering, Nanyang Technological University, 62 Nanyang Drive, Singapore 637459, Singapore. E-mail: xwlou@ntu.edu.sg; davidlou88@gmail.com

^c School of Materials Science and Engineering, Yeungnam University, Gyeongsan 712-749, Korea.

^d Department of Materials Science & Engineering, Zhejiang University, Hangzhou 310000, Zhejiang, China.

[‡] These authors contributed equally to this work.

* Corresponding authors

Experimental Section

Synthesis of Fe₂O₃ nanocubes: Fe₂O₃ nanocubes were synthesized through a simple precipitation method. In a typical synthesis, 50 mL of 5.4 M NaOH solution was added to 50 mL of 2.0 M FeCl₃ solution within 5 min under continuous stirring at 75 °C. The resultant Fe(OH)₃ gel was continually stirred at the same temperature for another 5 min, and was then kept at 100 °C in a preheated oven for 4 days. After cooling to room temperature naturally,

the red product was separated and washed by centrifugation with deionized water and ethanol for several times before drying at 70 °C overnight.

Synthesis of Fe₂O₃@PDA core-shell nanocubes: 80 mg of Fe₂O₃ nanocubes and 40 mg of dopamine hydrochloride were dispersed into 100 mL of Tris-buffer solution (10 mM) with magnetic stirring for 3 h. The resultant product was collected via centrifugation and washed with deionized water and ethanol for three times respectively, and dried at 70 °C overnight.

Synthesis of Fe₃O₄@C yolk-shell nanoboxes: The as-prepared Fe₂O₃@PDA core-shell nanocubes were first annealed at 500 °C for 3 h in Ar with a heating rate of 2 °C min⁻¹ to transform into Fe₃O₄@C core-shelled nanocubes. The annealed product was then dispersed in 4 M HCl solution with stable stirring. After an etching time of 45 min, Fe₃O₄@C-45 yolk-shell nanoboxes were harvested by several rinse-centrifugation cycles with DI water and ethanol, and dried at 70 °C overnight. The carbon nanoboxes were obtained by increasing the etching time to 6 h.

Synthesis of FeS₂@C yolk-shell nanoboxes: In a typical synthesis, the as-obtained Fe₃O₄@C powder and sulfur powder were loaded in the combustion boat with the sulfur totally submerging Fe₃O₄@C powders. A glass plate was partially covered on the combustion boat with the downstream side opening. Ar gas (500 sccm) was initially flowed into the tube for 1 hour to remove the air. Then, the samples were annealed at 400 °C for 3 h with a heating rate of 2 °C min⁻¹ under Ar atmosphere with a flow rate of 200 sccm. The FeS₂@C yolk-shelled nanoboxes were obtained after cooling to ambient temperature. The black solid products were rinsed with carbon disulfide and then harvested by centrifugation with DI water and ethanol for several times. Finally, the purified FeS₂@C nanomaterials are dried at 70 °C under vacuum state for 6 h. The FeS₂ particles without carbon shells were also synthesized by initially annealing Fe₂O₃ nanocubes at 500 °C for 3 h under a mixed gas of 95% Ar and 5% H₂. The following sulfidation process was the same to that for FeS₂@C.

Materials characterization: Field-emission scanning electron microscope (FESEM; JEOL

JSM07600F) and transmission electron microscope (TEM; JEOL JEM-2100F) were used to characterize the microscopic features of the samples. A Rigaku D/MAX RINT-2000 X-Ray Diffractometer with Cu K α radiation at a voltage of 40 kV and a current of 40 mA was used to collect the XRD patterns of the products. Thermogravimetric analysis (TGA) was performed with a temperature ramp of 10 °C min⁻¹ under air flow. The specific surface areas and pore volume of as-synthesized materials were measured using BET method on Autosorb-1 at liquid-nitrogen temperature.

Electrochemical measurements: The battery tests were carried out in a half-cell configuration. The working electrode consists of active materials, conductivity agent (Carbon black, CB), and polymer binder (polyvinylidene fluoride, PVDF) with a weight ratio of 70:20:10. The active mass loading on the electrode is about 1.2 mg cm⁻². The electrolyte was a solution of 1 M NaSO₃CF₃ in diethylene glycol dimethyl ether with 5 % fluoroethylene carbonate (FEC) additive. Sodium disc was used as both counter electrode and reference electrode. The coin-type half cells were assembled in argon-filled glove box and then tested in TOSCAT 3000 battery tester (TOSCAT 3000, Toyo Systems, Tokyo, Japan) with a voltage range between 0.1 and 2.0 V. Cyclic voltammetry (CV) curves were tested using AUTOLAB potentiostat/galvanostat apparatus (AUT85698) with a scan rate of 0.1 mV s⁻¹. The electrochemical impedance measurements were carried out at a 10 mV ac oscillation amplitude over the frequency range of 100 kHz to 100 mHz.

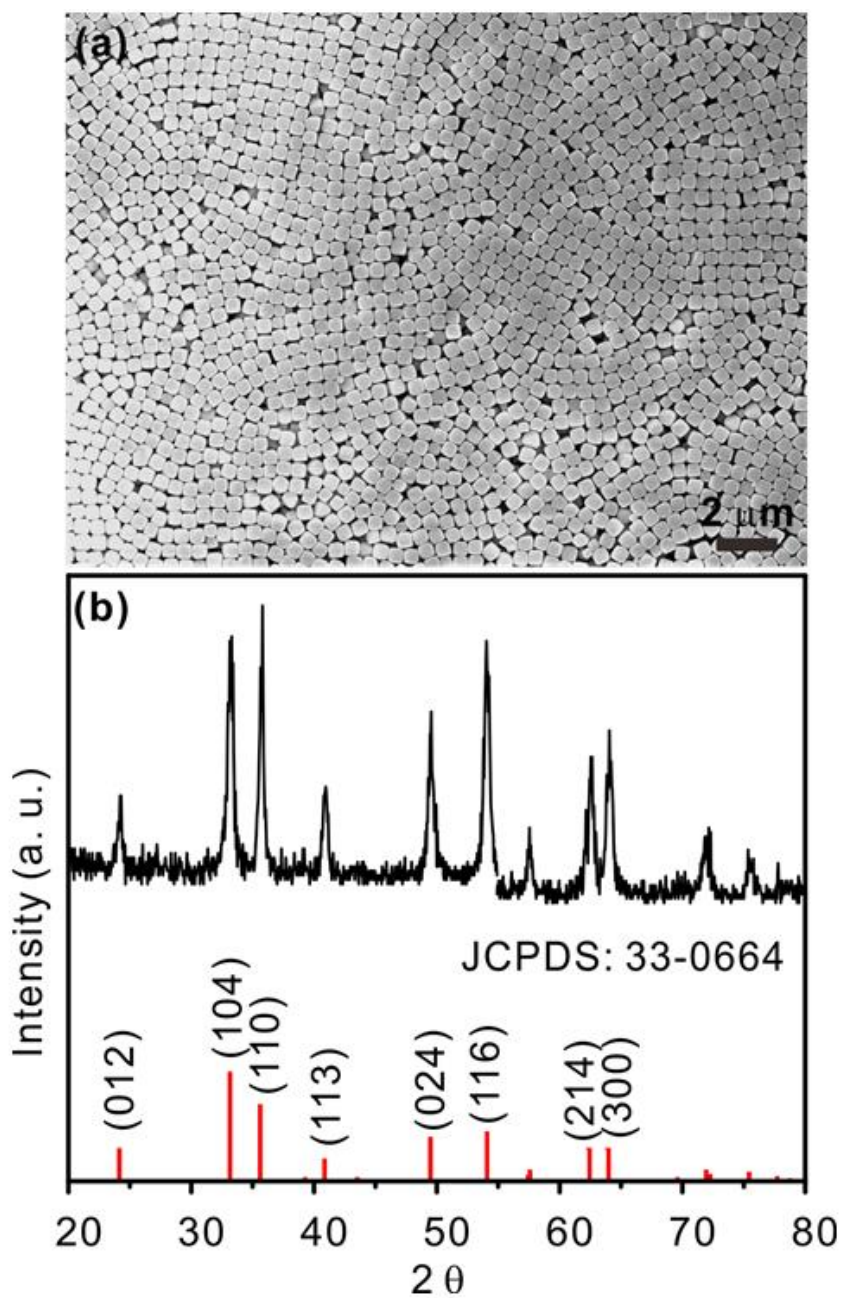


Fig. S1 (a) FESEM image and (b) XRD pattern of Fe₂O₃ nanocubes.

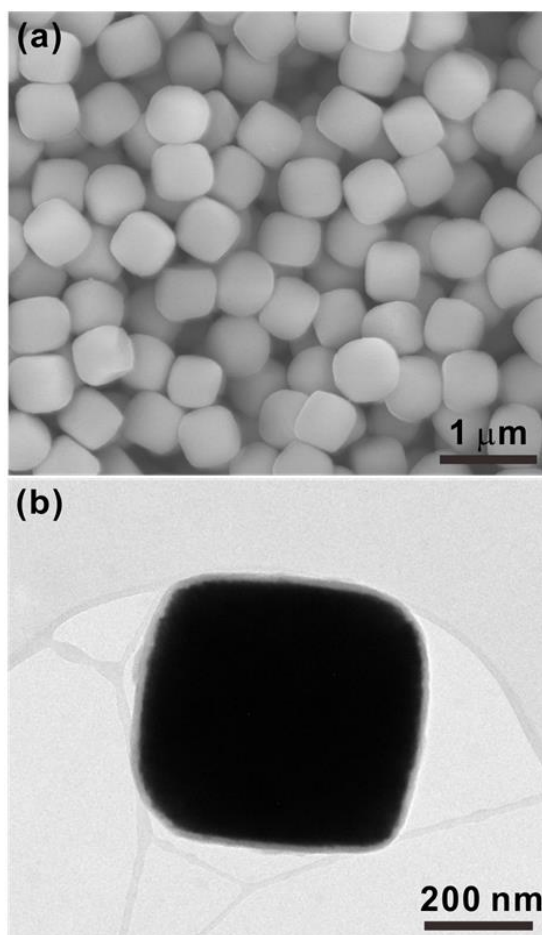


Fig. S2 (a) FESEM image and (b) TEM image of Fe_2O_3 @PDA core-shell nanocubes.

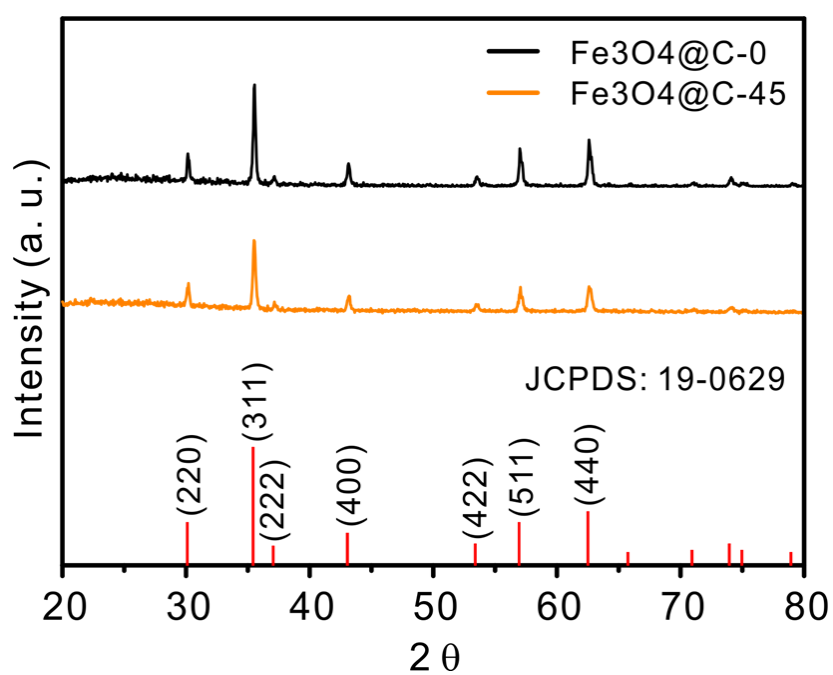


Fig. S3 XRD patterns of Fe_3O_4 @C-0 and Fe_3O_4 @C-45.

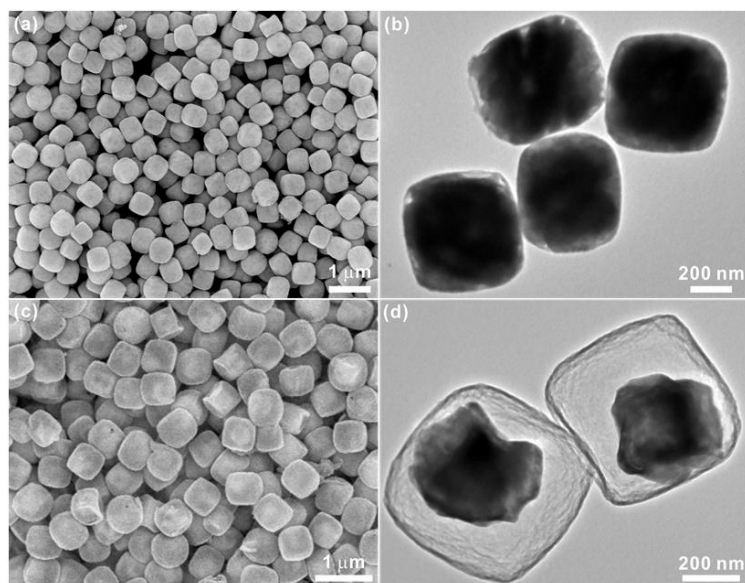


Fig. S4 FESEM and TEM images of Fe₃O₄@C-0 (a, b) and Fe₃O₄@C-45 (c, d).

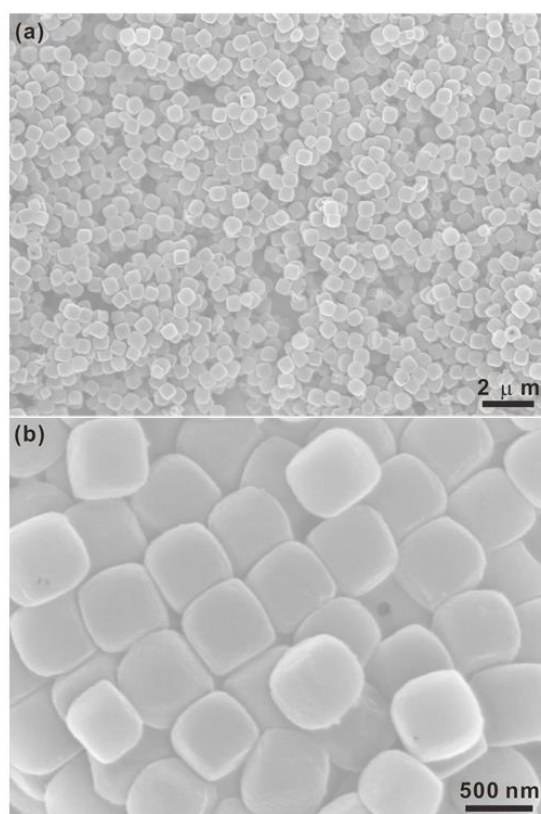


Fig. S5 FESEM images of carbon nanoboxes.

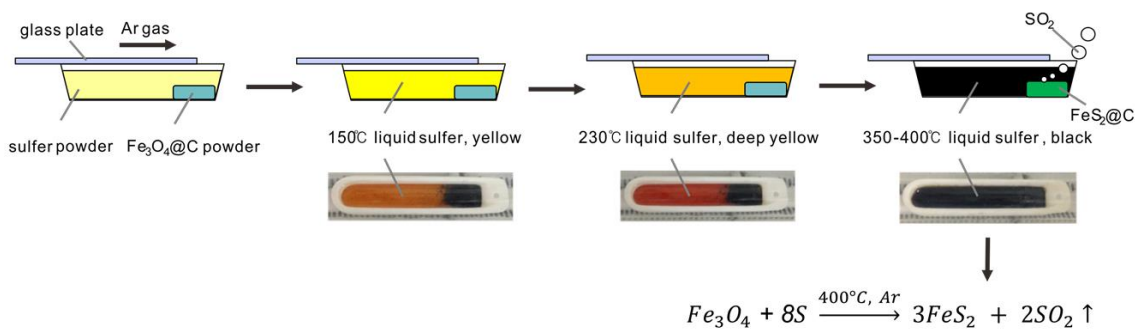


Fig. S6 Schematic illustration of the sulfidation process of $FeS_2@C-0$ and $FeS_2@C-45$.

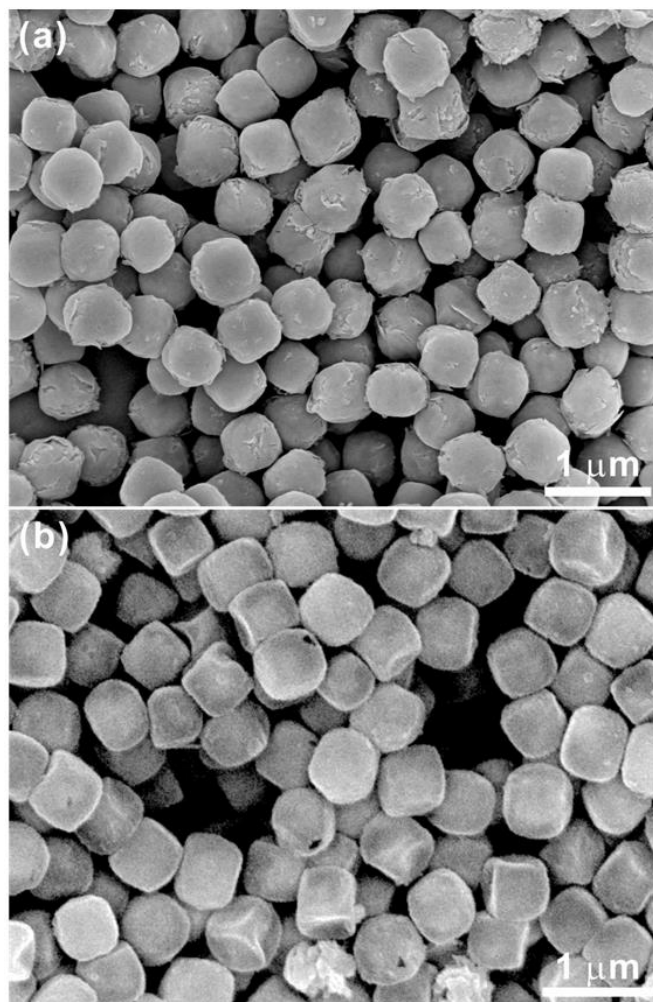


Fig. S7 FESEM images of $FeS_2@C-0$ (a) and $FeS_2@C-45$ (b).

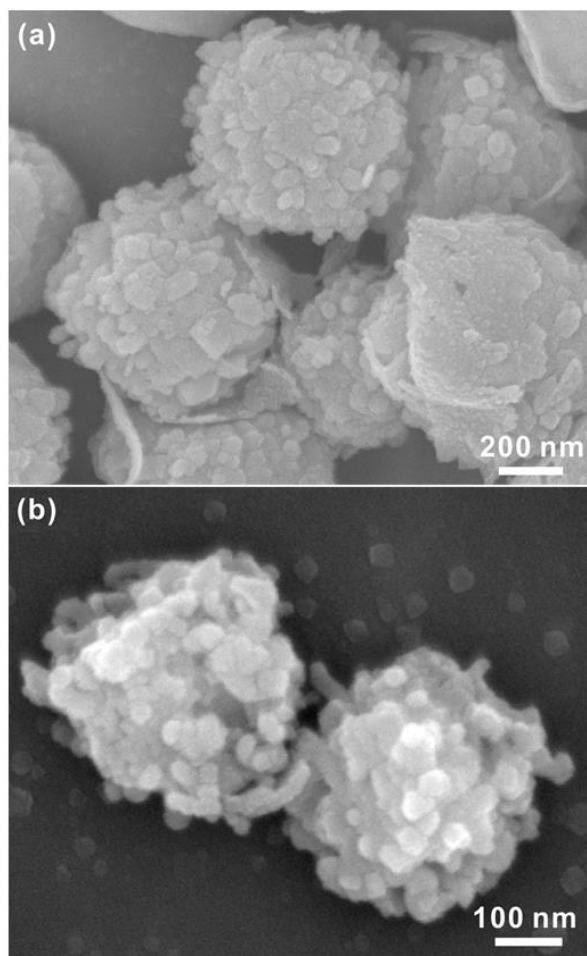


Fig. S8 FESEM images after sonication of FeS₂@C-0 (a) and FeS₂@C-45 (b).

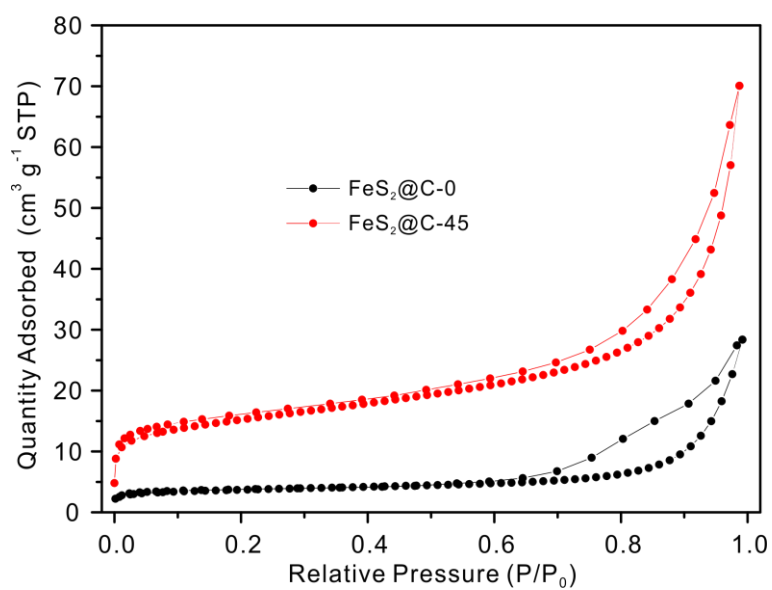


Fig. S9 Nitrogen adsorption-desorption isotherms of FeS₂@C-0 and FeS₂@C-45.

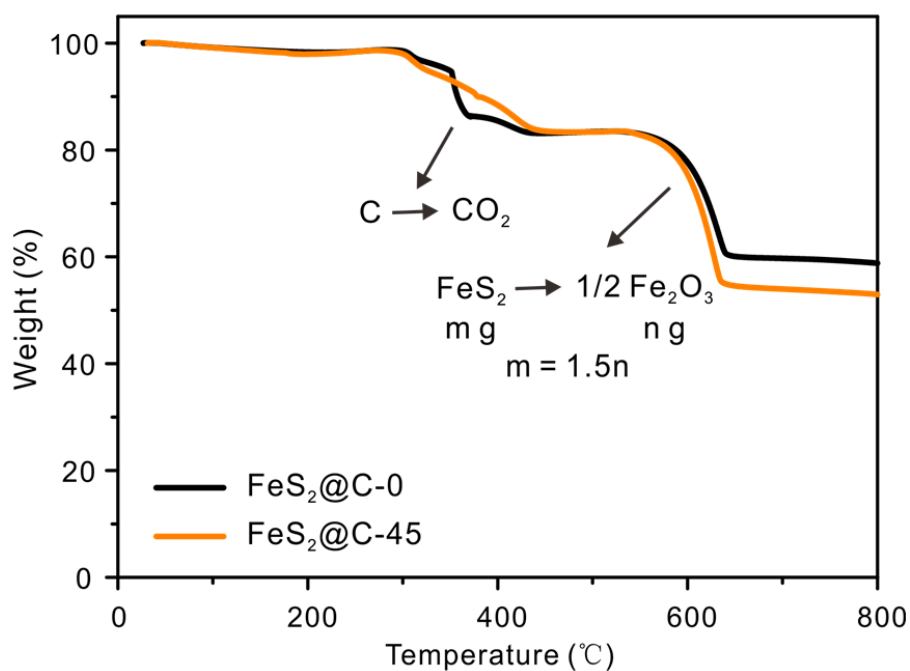


Fig. S10 TGA analysis of FeS₂@C-0 and FeS₂@C-45 at a temperature ramp of 10 °C min⁻¹ in air.

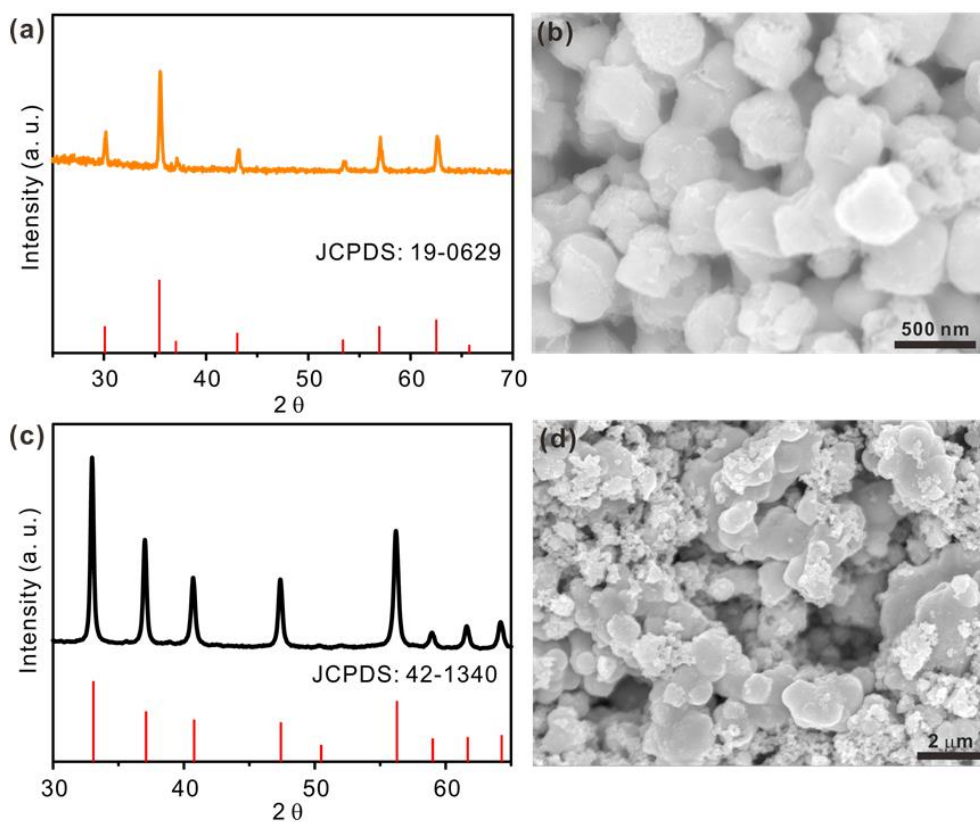


Fig. S11 (a) XRD pattern and (b) FESEM image of Fe₃O₄ particles; (c) XRD pattern and (d) FESEM image of FeS₂ particles.

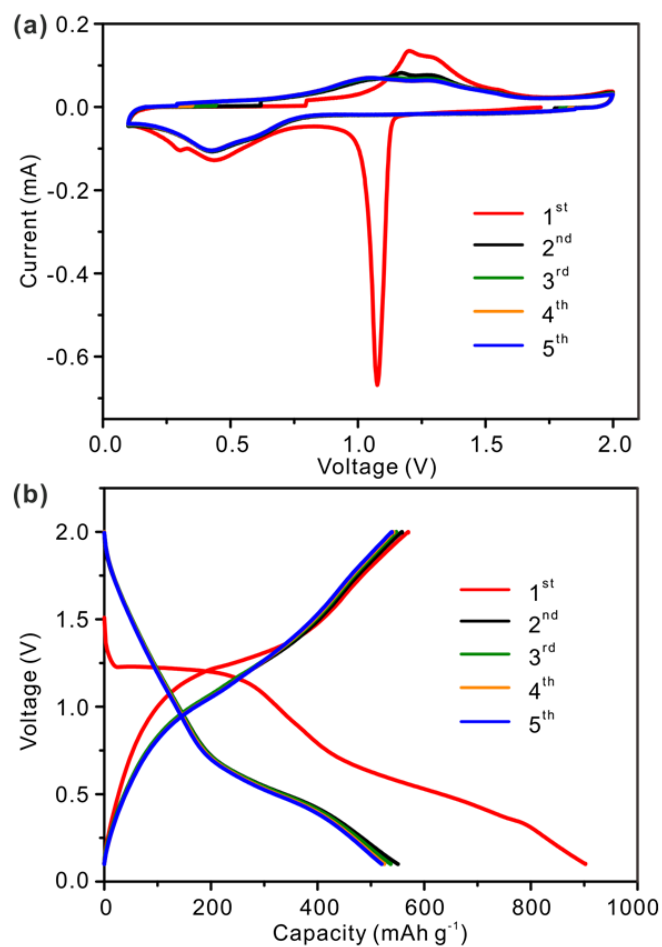


Fig. S12 (a) CV curves (at a scan rate of 0.1 mV s^{-1}) and (b) voltage profiles (at a current density of 100 mA g^{-1}) of FeS₂@C-0 for the first five cycles.

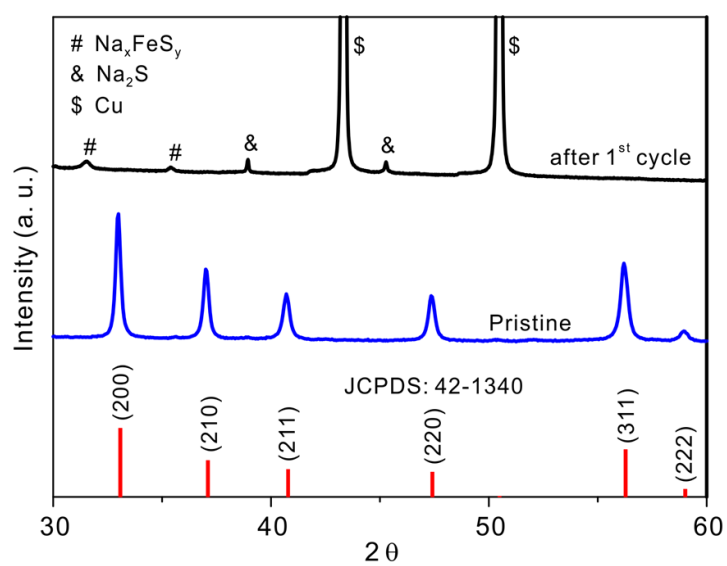


Fig. S13 XRD patterns of FeS₂ before and after the first cycle.

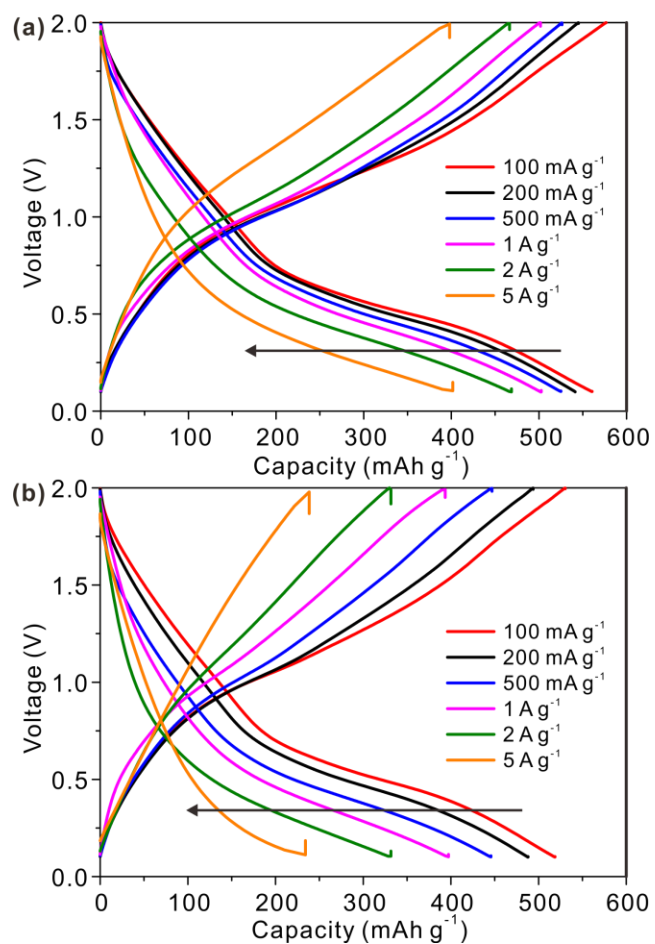


Fig. S14 The voltages profiles at various current densities of FeS₂@C-0 and FeS₂@C-45.

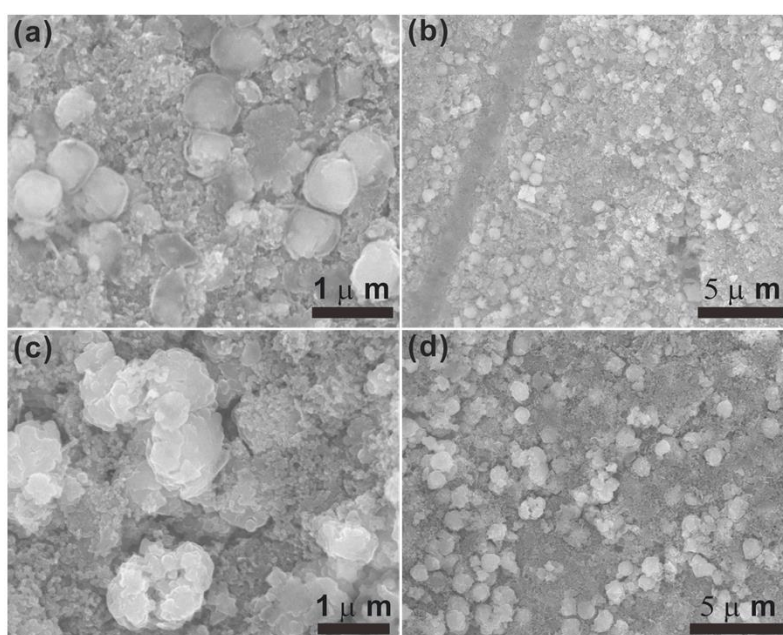


Fig. S15 FESEM images of FeS₂@C-45 (a, b) and FeS₂@C-0 (c, d) after rate-cycling at various current rates from 100 mA g⁻¹ to 5 A g⁻¹.

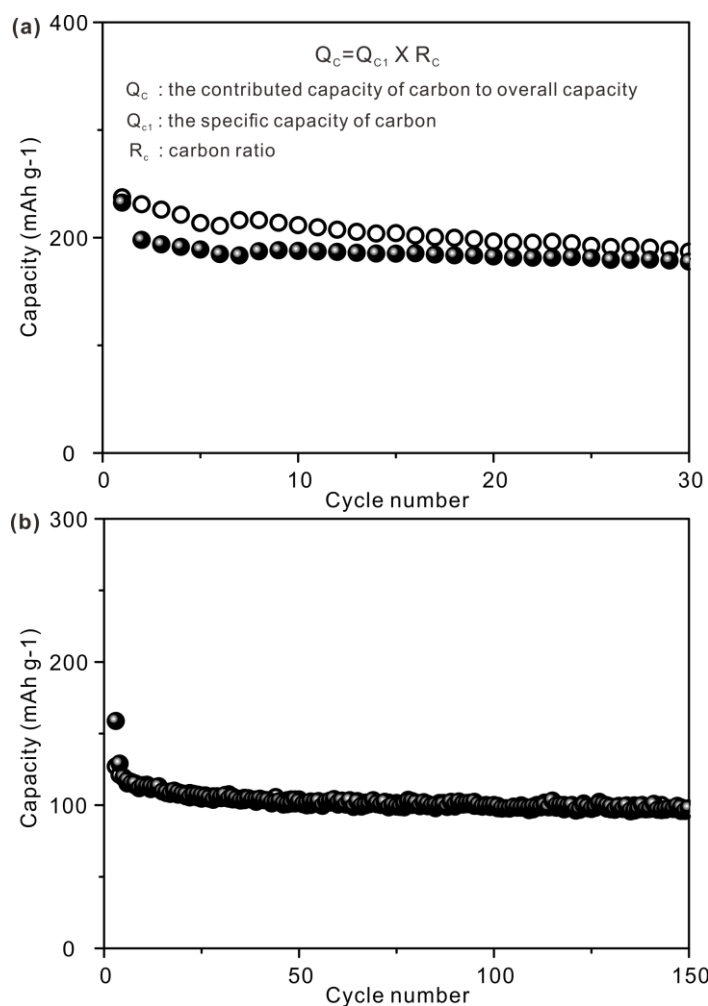


Fig. S16 The cycle performance of carbon nanoboxes at a current density of (a) 100 mA g⁻¹ and (b) 2 A g⁻¹, respectively.

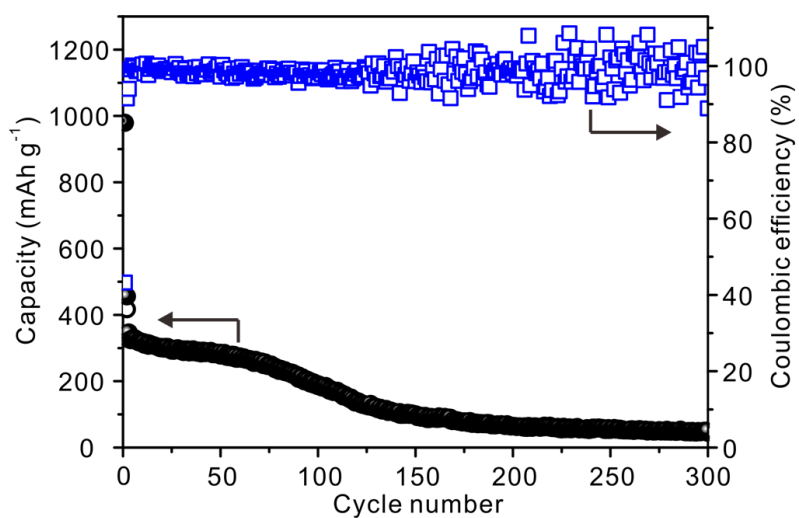


Fig. S17 The cycle performance of FeS₂ without carbon shells at a current density of 2 A g⁻¹.

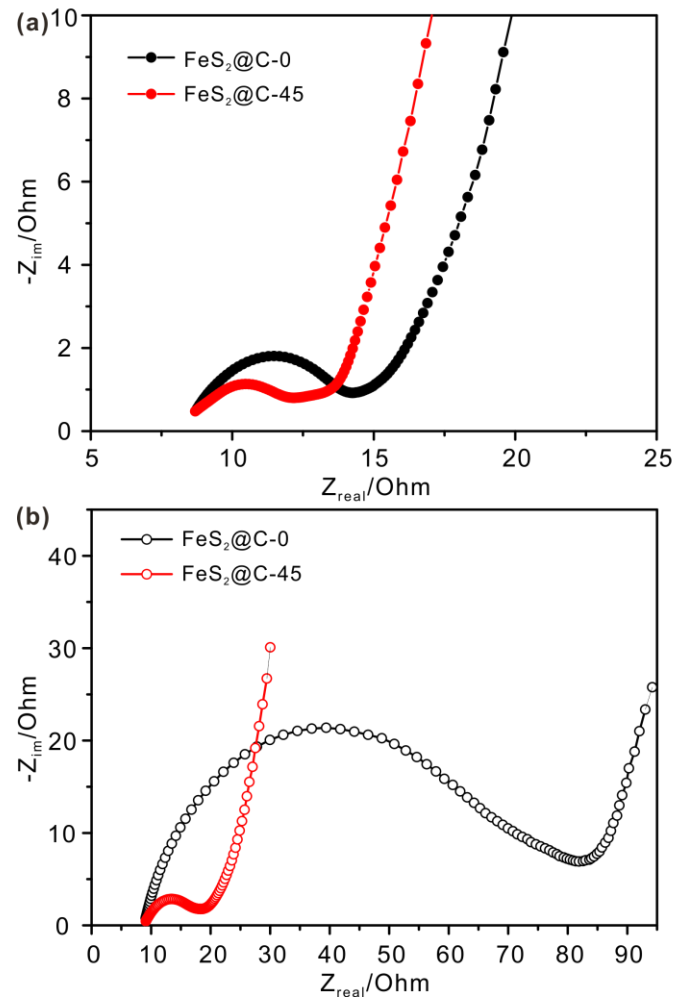


Fig. S18 Electrochemical Impedance Spectroscopy (EIS) of FeS₂@C-0 and FeS₂@C-45 (a) before cycling and (b) after 20 cycles.

Table S1. Comparison of some typical metal sulfide anode materials for SIBs.

Types of materials	Cycling performance	Rate capability	Ref.
SnS ₂ /Graphene	619 mAh g ⁻¹ after 100 cycles at 200 mA g ⁻¹	326 mAh g ⁻¹ at 4 A g ⁻¹	[1]
SnS ₂ /NGS	450 mAh g ⁻¹ after 100 cycles at 200 mA g ⁻¹	148 mAh g ⁻¹ at 10 A g ⁻¹	[2]
SnS/C	260 mAh g ⁻¹ after 300 cycles at 1 A g ⁻¹	145 mAh g ⁻¹ at 10 A g ⁻¹	[3]
CuS-rGO	393 mAh g ⁻¹ after 50 cycles at 100 mA g ⁻¹	345 mAh g ⁻¹ at 4 A g ⁻¹	[4]
Cu ₂ S	220 mAh g ⁻¹ after 20 cycles at 50 mA g ⁻¹	220 mAh g ⁻¹ at 50 mA g ⁻¹	[5]
Co ₃ S ₄ @polyaniline	253 mAh g ⁻¹ after 100 cycles at 200 mA g ⁻¹	184 mAh g ⁻¹ at 4 A g ⁻¹	[6]
Co ₉ S ₈ -C	404 mAh g ⁻¹ after 50 cycles at 500 mA g ⁻¹	326 mAh g ⁻¹ at 1.5 A g ⁻¹	[7]
CoS ₂ -MWCNT	568 mAh g ⁻¹ after 100 cycles at 100 mA g ⁻¹	449 mAh g ⁻¹ at 0.8 A g ⁻¹	[8]
Pyrite FeS ₂	180 mAh g ⁻¹ after 20000 cycles at 1 A g ⁻¹	170 mAh g ⁻¹ at 20 A g ⁻¹	[9]
Fe _{1-x} S/CNT	449 mAh g ⁻¹ after 200 cycles at 500 mA g ⁻¹	326 mAh g ⁻¹ at 8 A g ⁻¹	[10]
FeS-rGO	547 mAh g ⁻¹ after 50 cycles at 500 mA g ⁻¹	340 mAh g ⁻¹ at 6 A g ⁻¹	[11]
FeS@C/carbon cloth	430 mAh g ⁻¹ after 50 cycles at 91 mA g ⁻¹	280 mAh g ⁻¹ at 4.6 A g ⁻¹	[12]
FeS ₂ @C yolk-shell nanobox	511 mAh g ⁻¹ after 100 cycles at 100 mA g ⁻¹	560 mAh g ⁻¹ at 100 mA g ⁻¹	Present work
	330 mAh g ⁻¹ after 800 cycles at 2 A g ⁻¹	403 mAh g ⁻¹ at 5 A g ⁻¹	

Supplementary References

- [1] Y. C. Liu, H. Y. Kang, L. F. Jiao, C. C. Chen, K. Z. Cao, Y. J. Wang, H. T. Yuan, *Nanoscale*, 2015, **7**, 1325.
- [2] Y. Jiang, Y. Z. Feng, B. J. Xi, S. S. Kai, K. Mi, J. K. Feng, J. H. Zhang, S. L. Xiong, *J. Mater. Chem. A*, 2016, **4**, 10719.
- [3] C. B. Zhu, P. Kopold, W. H. Li, P. A. van Aken, J. Maier, Y. Yu, *Adv. Sci.*, 2015, **2**, 1500200.
- [4] J. Li, D. Yan, T. Lu, W. Qin, Y. Yao, L. Pan, *ACS Appl. Mater. Interfaces*, 2017, **9**, 2309.
- [5] H. S. Kim, D. Y. Kim, G. B. Cho, T. H. Nam, K. W. Kim, H. S. Ryu, J. H. Ahn, H. J. Ahn, *J. Power Sources*, 2009, **189**, 864.
- [6] Q. Zhou, L. Liu, Z. F. Huang, L. G. Yi, X. Y. Wang, G. Z. Cao, *J. Mater. Chem. A*, 2016, **4**, 5505.
- [7] Y. N. Ko, Y. C. Kang, *Carbon*, 2015, **94**, 85.
- [8] Z. Shadike, M. H. Cao, F. Ding, L. Sang, Z. W. Fu, *Chem. Commun.*, 2015, **51**, 10486.
- [9] Z. Hu, Z. Q. Zhu, F. Y. Cheng, K. Zhang, J. B. Wang, C. C. Chen, J. Chen, *Energy Environ. Sci.*, 2015, **8**, 1309.
- [10] Y. Xiao, J. Y. Hwang, I. Belharouak, Y. K. Sun, *ACS Energy Lett.*, 2017, **2**, 364.
- [11] S. Y. Lee, Y. C. Kang, *Chem. Eur. J.*, 2016, **22**, 2769.
- [12] X. Wei, W. H. Li, J. A. Shi, L. Gu, Y. Yu, *ACS Appl. Mater. Interfaces*, 2015, **7**, 27804.